Geomechanics and Engineering, *Vol. 26, No. 5 (2021) 453-464*
https://doi.org/10.12989/gae.2021.26.5.453

Modified pseudo-dynamic analysis of rigid gravity retaining wall with cohesion-less backfill and uniform surcharge

Godas Srikar* and Satyendra Mittal[a]

Department of Civil Engineering, Indian Institute of Technology Roorkee, Roorkee, Uttarakhand-247667, India

(Received June 2, 2020, Revised May 24, 2021, Accepted August 30, 2021)

Abstract. An increase in failure of geotechnical structures is a significant concern in seismic-prone areas. The purpose of the study is to propose a closed-form solution for the seismic active pressure acting on a retaining wall with backfill subjected to uniform surcharge considering the propagation of both shear and primary waves. The proposed study considers the damping ratio by assuming soil as Kelvin-Voigt material. The proposed methodology satisfies boundary conditions at the surface of the backfill due to surcharge. The deduced acceleration profile is considered for the estimation of inertial forces due to critical wedge and surcharge. The study reveals that the maximum seismic active pressure coefficient occurs when the normalized input frequency is equal to $\pi/2$. It is observed that the surcharge magnitude does not affect both horizontal and vertical acceleration profiles. The parametric study presents the influence of various static and dynamic properties of the backfill soil on the distribution of seismic pressure acting on the wall. The coefficient of earth pressure obtained from the proposed method is in good agreement with the existing pseudo-static methods. It is concluded that the effect of shear wave propagation on earth pressure is relatively dominant as compared to that of primary wave propagation.

Keywords: active pressure; damping ratio; modified pseudo-dynamic analysis; primary wave velocity; shear wave velocity; surcharged backfill

1. Introduction

The important criterion for the design of a retaining wall is its stability against overturning and sliding of the wall. The predominant force causing the overturning and sliding is total active thrust acting on the wall due to retained backfill soil. The safe design of the retaining wall requires the precise estimation of lateral earth pressure acting on the wall and it leads to complexity when additional seismic forces are applied.

A very simple and linear approach has been in practice for estimating lateral earth pressure under seismic conditions. In this method, the seismic load is approximated as an additional static load in the free body diagram of a critical wedge. Therefore this method is termed as pseudo-static method (Okabe (1924) and Mononobe and Matsuo (1929)). This method is the pioneering method that solved problems related to seismic earth pressure for decades due to its simplistic nature of the solution. Considering the pseudo-static method, many variants of the studies have been present by the researchers (Richards and Elms (1979), Zhang *et al.* (2019), Huang and Liu (2016)). Besides a simplistic methodology, the pseudo-static method has various approximations. The dynamic load due to seismic action is considered a simple time-invariant load. The propagation of shear and primary waves in backfill media has been neglected. The method results in a linear earth pressure distribution for both static and seismic cases.

In an attempt to include the dynamic nature in the earth pressure-related problems, Steedman and Zeng (1990) proposed a pseudo-dynamic method. The uncertainties in the pseudo-static method have been addressed and time-dependent seismic inertial force is considered. Choudhury and Nimbalkar (2006) improvised the pseudo-dynamic method considering vibrations in both horizontal and vertical directions by considering a finite shear wave velocity and primary wave velocity. A linear acceleration amplification is also considered as the seismic wave propagates in the backfill. Different researchers have studied various variants of the pseudo-dynamic method. Kolathayar and Ghosh (2009), Ghosh (2008), Ghosh (2010), Ghanbari and Ahmadabadi (2010) proposed the effect of acceleration amplification on the earth pressure acting behind a battered retaining wall. Baziar *et al.* (2013), Nimbalkar and Choudhury (2007), Choudhury and Nimbalkar (2007) adopted the pseudo-dynamic method to estimate the stability of the retaining wall and compared the study with the pseudo-static method. The study concluded that the pseudo-dynamic method is an advisable method for the higher seismic coefficients. Qin and Chian (2018) have applied the same methodology to analyze the reinforced retaining wall. The efficacy of the analysis can be optimized by performing a reliability analysis (Hu and Huang (2019)). Various researchers also employed the Finite Element Method (FEM) to capture the dynamic behavior of cantilever retaining wall (di Santolo and Evange- lista (2011), Evangelista *et al.* (2010), Cakir (2013), Cakir

*Corresponding author, Senior Research Fellow
E-mail: gsrikar@ce.iitr.ac.in
[a]Professor
E-mail: satyendramittal@gmail.com

ISSN: 2005-307X (Print), 2092-6219 (Online)

(2014a), Cakir (2014b), Kloukinas *et al.* (2015)). Finite element analysis is applied to take advantage of applying both harmonic and transient excitation (Veletsos and Younan (1994a), Cakir and Livaoglu (2013)). It is evident that the flexibility of retaining wall plays an important role in seismic design of retaining walls as the point of application of seismic lateral thrust changes with the flexibility of retaining wall (Psarropoulos *et al.* (2005), Giarlelis and Mylonakis (2011), Gazetas *et al.* (2004), Madabhushi and Zeng (2007)).

The pseudo-dynamic method has many advantages over that of a pseudo-static approach and it also has demerits. The Pseudo-dynamic method does not satisfy the zero-stress condition at the surface of the backfill. The pseudo-dynamic method considers the shear wave velocity of the backfill material but fails to consider the damping resistance offered by the backfill material to the applied seismic wave. For the problems related to dynamic loading, it is appropriate to model soil as a visco-elastic material (Veletsos and Younan (1994b), Veletsos and Younan (1997)). Bellezza (2014) proposed a modified pseudo-dynamic method based on the analysis proposed by Veletsos and Younan (1994b), Veletsos and Younan (1997). The boundary conditions due to propagating seismic waves in the backfill at rigid base and surface are satisfied. Different variants have been proposed by the researchers based on the modified pseudo-dynamic method (Annapareddy and Pain (2019), Pain *et al.* (2018), Pain *et al.* (2017)). Pain *et al.* (2017) applied the modified pseudo-dynamic method to check the stability of the retaining wall against rotation for dry backfill conditions. Cakir (2017), Taravati and Ardakani (2018) performed numerical analysis to study the behavior of retaining walls for the applied dynamic loading.

The presence of surcharge on the surface of the backfill is a common practical scenario. Seismic analysis of retaining wall with the surcharge on the backfill is presented by various researchers. Motta (1994) had proposed a limit equilibrium analysis to estimate the earth-pressure coefficient considering the seismic effect by the pseudo-static method. Choudhury and Rao (2002) have proposed passive resisting force acting on the wall with surcharged backfill by considering the negative soil-wall friction. Kumar and Chitikela (2002) and Santhoshkumar and Ghosh (2018) proposed method of stress characteristics to estimate total lateral earth pressure from a coupled solution of surcharge component and unit weight components. However, Santhoshkumar and Ghosh (2020) had proposed the decoupled effect to surcharge and unit weight components, assumed a negligible effect of surcharge on horizontal and vertical acceleration profiles. Greco (2006) extended Coulomb's solution to the backfill subjected to line surcharge. Caltabiano *et al.* (2000) have proposed the modified limit equilibrium analysis of retaining wall with surcharged backfill by considering the presence of the wall in equilibrium equations. Mylonakis *et al.* (2007) had proposed a stress plasticity solution wherein a single closed-form solution gives both active and passive pressures. In practical applications of the retaining wall, the most common observation is that the retaining wall is subjected to seepage forces. Wang *et al.* (2008) investigated the passive earth pressure acting on the retaining wall subjected to seepage pressure due to the upward and downward flow of water in the surcharged backfill. Apart from this, Shukla (2013) had proposed a closed-form solution to estimate the effect of cohesion on the lateral earth pressure acting on the retaining wall with surcharged backfill. Sahoo and Ganesh (2017) have proposed a limit analysis considering a composite collapse mechanism for the analysis of retaining wall with backfill subjected to an inclined surcharge. The limit analysis is adopted by Aminpour *et al.* (2017) to estimate the permanent displacement of soil slope with a surcharge for both translation and rotation modes of failure. Srikar and Mittal (2020) proposed modified pseudo-dynamic method to estimate the seismic coefficient of lateral earth pressure considering uniform surcharge. Motlagh *et al.* (2018) has proposed a new procedure to estimate the effect of surcharge on tensile strength and length of the reinforcement for a slope under pseudo-static conditions.

The available literature shows that the pseudo-static method is considered to study the effect of surcharge on lateral earth pressure distribution under dynamic conditions, which leads to multiple limitations: 1. The effect of amplification of shear wave and primary wave on lateral pressure distribution in the presence of surcharge is not explored. 2. The boundary stress condition due to the presence of surcharge on the surface of the backfill is neglected by the propagating wave. 3. The time and frequency-dependent inertial forces induced due to surcharge at the surface of the backfill are neglected. These limitations are addressed by proposing a closed-form solution to estimate total active thrust acting on an inclined retaining wall. Novelty in the study majorly lies in satisfying the boundary condition due to the presence of surcharge and considering time-dependent inertial forces due to surcharge. The influence of different seismic properties (input frequency of the shear wave and primary wave, damping ratio horizontal and vertical seismic coefficient) and static properties (angle of shearing resistance, soil-wall friction, wall-inclination) on lateral earth pressure distribution is pre sented. The effectiveness of the present study is established by comparing the results obtained from the proposed study with that of the existing pseudo-static and pseudo-dynamic methods

2. Methodology

Fig. 1 shows a retaining wall of height H with backfill subjected to a uniform surcharge of intensity q from the face of the wall. It is assumed that the retaining wall is battered at an angle 'ϵ' with vertical. The backfill material is assumed to be cohesion-less soil with an angle of internal friction 'ϕ'. It is assumed that the soil-wall system is resting on the rigid bedrock, ensuring that no failure is induced due to the base.

The bedrock is subjected to harmonic excitation. In existing pseudo-static or pseudo-dynamic methods, the soil is considered a linear-elastic material. But real materials

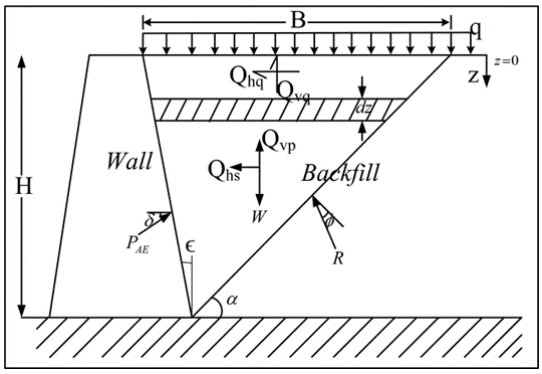

Fig. 1 Free body diagram of potential failure wedge adjacent to the wall

dissipate the energy due to the propagation of seismic waves due to the damping phenomenon. Therefore, instead of assuming soil as a linear elastic material, it is reasonable to assume it as visco-elastic material for dynamic problems. So, the backfill material is modeled as Kelvin-Voight visco-elastic material where some part of shearing deformation is resisted by elastic component and the other by viscous component. The present study considers the propagation of both the shear wave and the primary wave. V_s, V_p be the shear wave velocity and primary wave velocity of the backfill material, respectively.

For a Kelvin-Voight material, the governing equations of motion are as follows Kramer (1996)

$$\rho\frac{\partial^2 u_h}{\partial t^2}=G\frac{\partial^2 u_h}{\partial z^2}+\eta_s\frac{\partial^3 u_h}{\partial z^3\partial t} \tag{1}$$

$$\rho\frac{\partial^2 u_v}{\partial t^2}=(\lambda+2G)\frac{\partial^2 u_v}{\partial z^2}+(\eta_1+2\eta_s)\frac{\partial^3 u_v}{\partial z^3\partial t} \tag{2}$$

Eq. (1) and Eq. (2) are the differential equations in terms of horizontal displacement and vertical displacement, respectively. The general solution in terms of displacement is obtained by satisfying the

boundary conditions due to surcharge at the surface of the backfill and displacement due to horizontal and vertical components of the shaking due to bed-rock motion.

Displacement in terms of shear wave velocity (V_s) and damping resistance (ξ_s) of backfill due to horizontal harmonic excitation with frequency (ω_s) is obtained by considering boundary constraint as shear stress at backfill surface $\tau=q\tan(\phi)$, the horizontal component of the vibration at the base as $u_{hb}=u_{ho}\cos(\omega_s t)$.

$$u_h(z,t)=X+\frac{u_{h0}}{U_s^2+V_s^2}\left[(U_sU_{sz}+V_sV_{sz})\cos\omega_s t+(V_sU_{sz}-U_sV_{sz})\sin\omega_s t\right] \tag{3}$$

The acceleration of upward propagating shear wave is obtained by double differentiating Eq. (3) in the time domain as shown in Eq. (4).

$$a_h(z,t)=\frac{a_{h0}}{U_s^2+V_s^2}\left[(U_sU_{sz}+V_sV_{sz})\cos\omega_s t+(V_sU_{sz}-U_sV_{sz})\sin\omega_s t\right] \tag{4}$$

Similarly, the acceleration of propagating primary wave is also obtained by considering appropriate boundary conditions. The constraints adopted are normal stress at backfill surface $\sigma_n=q$, displacement due to harmonic excitation at the base rock $u_{vb}=u_{vo}*\cos(\omega_p t)$.

$$u_v(z,t)=Y+\frac{u_{v0}}{U_p^2+V_p^2}\left[(U_pU_{pz}+V_pV_{pz})\cos\omega_p t+(V_pU_{pz}-U_pV_{pz})\sin\omega_p t\right] \tag{5}$$

The acceleration of upward propagating primary wave is obtained by double differentiating Eq. (5) in the time domain as shown in Eq. (6).

$$a_v(z,t)=\frac{a_{v0}}{U_p^2+V_p^2}\left[(U_pU_{pz}+V_pV_{pz})\cos\omega_p t+(V_pU_{pz}-U_pV_{pz})\sin\omega_p t\right] \tag{6}$$

The terms used in horizontal displacement and horizontal acceleration are presented in Appendix A.1. The terms used in vertical displacement and vertical acceleration are presented in Appendix A.2.

In contrast to conventional methods, the obtained expressions for acceleration (horizontal and vertical) are the functions of shear wave velocity (V_s), primary wave velocity (V_p), Damping ratio of backfill material (ξ_s, ξ_p), frequency of shear wave (ω_s) and primary waves (ω_p) as shown in Eqs. (4) and (6). It also incorporates the effect of amplification without introducing any other factor, unlike existing pseudo-dynamic methods (Steedman and Zeng (1990)).

Fig. 1 shows a critical failure wedge assumed with a slip surface making an angle α with the horizontal. A small elemental strip of thickness '*dz*' is considered at depth z from the surface of the backfill. This element is subjected to the horizontal inertial force due to the shear wave and the vertical inertial force due to the primary wave. The inertial forces are obtained by integrating that of the elemental strip, as shown in Eqs. (7) and (8). The obtained equations depend on the inclination of the failure plane and time.

$$Q_{hs}(t,\alpha)=\int_0^H\left\{a_h(z,t)\frac{\gamma(H-z)}{g\tan\alpha}(\tan\varepsilon+\cot\alpha)\right\}dz \tag{7}$$

$$Q_{vp}(t,\alpha)=\int_0^H\left\{a_v(z,t)\frac{\gamma(H-z)}{g\tan\alpha}(\tan\varepsilon+\cot\alpha)\right\}dz \tag{8}$$

Application of surcharge on the backfill results in the inertial force due to amplified shear wave and primary wave. Unlike existing pseud-static studies, the present study allows estimating time-varying inertial forces due to surcharge. To estimate the amplification of the shear and primary waves, the acceleration is estimated at the surface of the backfill using Eqs. (4) and (6) and the obtained acceleration is multiplied to surcharge force as shown in Eqs. (9) and (10).

$$Q_{hq}=k_{ho}qH(\tan\varepsilon+\cot\alpha)\frac{(U_s\cos\omega_s t+V_{sh}\sin\omega_s t)}{U_s^2+V_{sh}^2} \tag{9}$$

$$Q_{vq}=k_{vo}qH(\tan\varepsilon+\cot\alpha)\frac{qH(U_p\cos\omega_p t+V_{pr}\sin\omega_p t)}{U_p^2+V_{pr}^2} \tag{10}$$

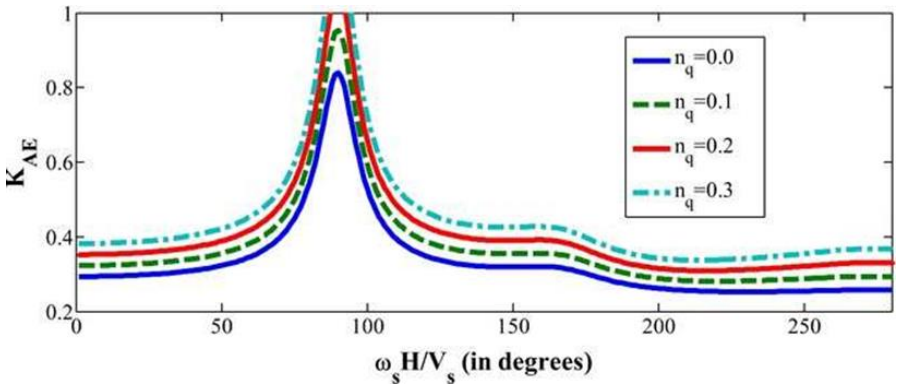

Fig. 2 Variation of seismic coefficient of earth pressure for a range of normalized frequency of shear wave

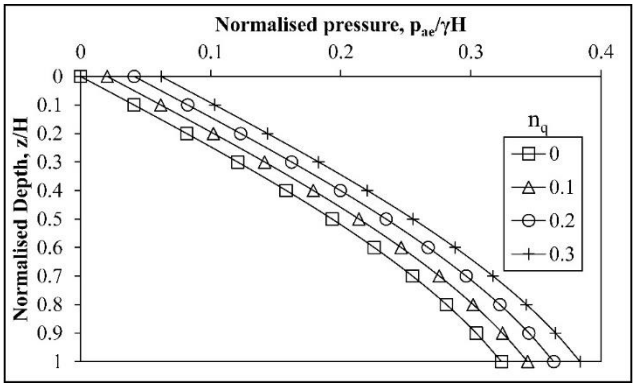

Fig. 3 Seismic active pressure for varying surcharge magnitudes

Positive magnitude is assumed when horizontal inertial force is pointed left and vertical inertial force is pointed upwards. Here, it is worth mentioning that the assumption of linear failure surface is not appropriate but, the present study emphasizes the proposed methodology in the presence of uniform surcharge. However, this assumption is adopted by many researchers, more importantly, for active earth pressure cases (Caltabiano *et al.* (2000), Motta (1994), Shukla (2013)). The forces exerted on the critical wedge are self-weight of the wedge, uniform surcharge, inertial force due to failure wedge and surcharge. The total active force (static and seismic) acting on the retaining wall is obtained from the equilibrium of forces as shown below

$$P_{AE}(\alpha,t)=\frac{1}{\cos(\delta-\alpha+\phi+\varepsilon)}\begin{Bmatrix}(W+qH(\tan\varepsilon+\cot\alpha))\sin(\alpha-\phi)\\+(Q_{hs}+Q_{hq})\cos(\alpha-\phi)\\-(Q_{vp}+Q_{vq})\sin(\alpha-\phi)\end{Bmatrix} \quad (11)$$

$$K_{AE}=\frac{2P_{AE,max}}{\gamma H^2} \quad (12)$$

$$p_{AE}(z,\alpha,t)=\frac{dP_{AE}(\alpha,t)}{dz} \quad (13)$$

The obtained seismic active thrust is the function of time and angle made by the rupture plane. Similar to pseudo-static and pseudo-dynamic methods, the total active thrust is normalized by considering the coefficient of seismic earth pressure, as shown in Eq. (12). Lateral seismic pressure distribution acting on the wall is determined by differentiating active thrust expression with respect to the varying depth z, as shown in Eq. (13).

3. Results and discussion

In this section of the paper, results related to the magnitude of the surcharge are presented. This section also presents a detailed study of parameters that influence lateral earth pressure. MATLAB script is developed to optimize the seismic coefficient of active thrust with respect to the angle made by failure plane and time (t/T) by varying from 1° to 89° and 0.0 to 1.0 respectively. In the present analysis, the primary wave velocity is assumed to be 1.87 times the shear wave velocity, which is appropriate for geological materials (Das (1993), Kramer (1996)) and equal damping ratio of backfill due to shear wave and primary wave ($\xi_s = \xi_p = \xi$).

Fig. 2 shows a plot between the normalized input frequency and the seismic coefficient of active thrust for different surcharge coefficients ($n_q = 2q/\gamma H$) varying from 0.0 to 0.3. The other parameters considered for the study are the base acceleration coefficient $k_{ho} = 0.1$, friction angle $\phi = 35°$, soil-wall friction $\delta = 0.5\phi$, $\omega_p/\omega_s = 1.0$. As expected, the value of the coefficient increases with an increase in surcharge magnitude. An important observation in the plot is that there is a sudden increase in the lateral coefficient at input frequency $\omega_s H/V_s = \pi/2$, i.e., at the first mode of vibration. The peak value of the coefficient reached depends on the magnitude of the uniform surcharge.

Fig. 3 shows lateral earth pressure acting on the wall for

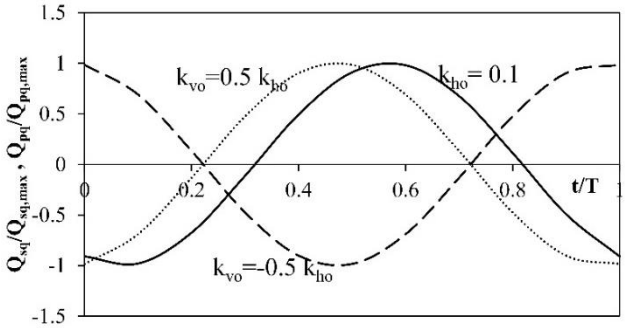

Fig. 4 Variation of surcharge inertial force with time

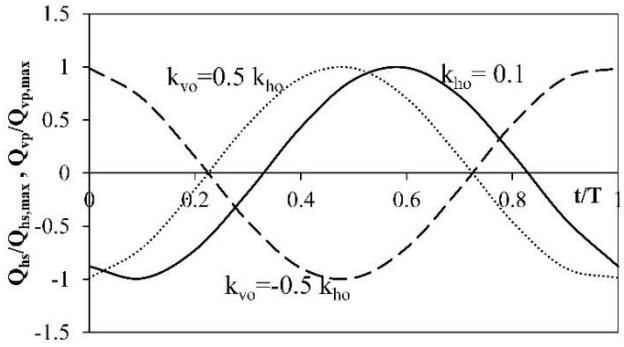

Fig. 5 Variation of inertial force due to soil wedge with time

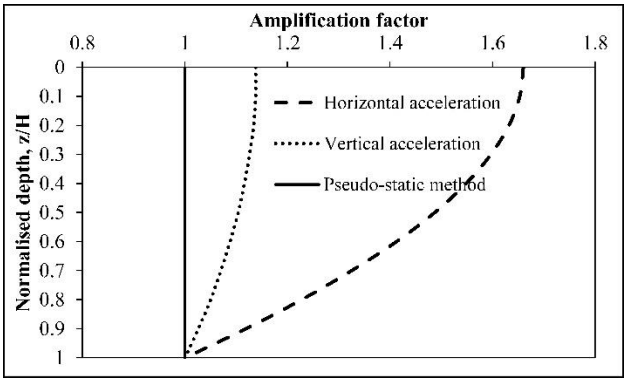

Fig. 6 Variation of Amplification factor for the normalized height of the retaining wall

different surcharge coefficients (n_q) varying from 0.0 to 0.3. Invariant parameters considered in the analysis are horizontal base acceleration coefficient k_{ho} = 0.1, vertical base acceleration coefficient k_{vo} = 0.5k_{ho}, damping resistance ξ = 10%, soil friction angle ϕ = 35°, soil-wall friction δ/ϕ = 0.5, normalized input frequency of shear wave $\omega_s H/V_s$ = 2.0, the ratio of the frequency of the shear wave to primary wave ω_p/ω_s = 1.0.

The plot shows a non-linear pattern of variation of pressure distribution. As the surcharge coefficient increases, earth pressure acting on the wall also increases without any change in the non-linearity in the curve.

Fig. 4 and Fig. 5 show the variation of normalized inertial force mobilized due to the surcharge and weight of the soil wedge with time (t/T), respectively, for k_{ho} = 0.1, k_{vo} = +0.5k_{ho}, and k_{vo} = −0.5k_{ho}.

The other parameters used in the analysis are soil friction angle ϕ = 35°, soil-wall friction δ/ϕ = 0.5,

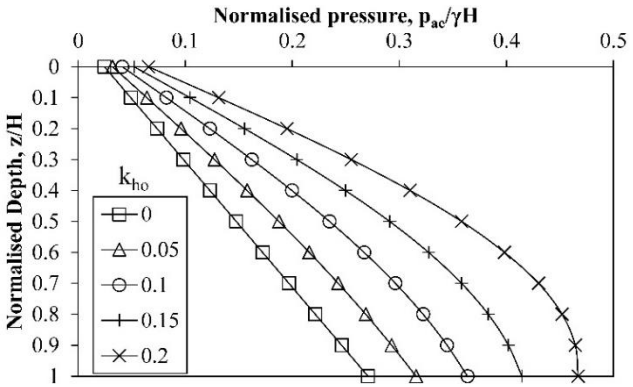

Fig. 7 Earth pressure distribution for different horizontal base acceleration coefficients

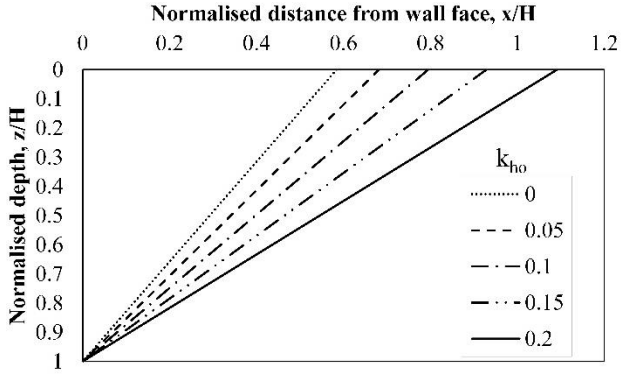

Fig. 8 Failure planes generated for different horizontal base acceleration coefficients

surcharge coefficient n_q = 0.2, $\omega_s H/V_s$ = 2.0, ω_p/ω_s = 1.0 and damping resistance ξ = 10%. From the plots, it is evident that the vertical inertial force and horizontal inertial force reach a maximum at different times. The obtained curves for inertial force due to surcharge and weight of the soil wedge are almost identical as the average value of wedge inertial force is considered in Fig. 5.

Fig. 6 shows the variation of amplification factor throughout the depth of the retaining wall. The amplification factor is the ratio of the acceleration obtained from Eq. 4 and 6 to the respective base accelerations. In the present variation, base horizontal accelerations k_{ho} is taken as 0.1 and base vertical acceleration is taken as 0.5k_{ho}. It is evident that the amplification due to horizontal acceleration is about 1.65 i.e., the base horizontal acceleration is increased by about 1.65 times on reaching the surface of the backfill. Similarly, the vertical acceleration is increased by 1.14 times as it reaches the surface of the backfill. In the present study, the amplification is directly obtained for the considered shear wave velocity, damping ratio of the backfill soil, input frequency of shear and primary waves. Fig. 6 also presents unit amplification for the case of the pseudo-static method, which implies that a constant value of the seismic coefficient is assumed throughout the height of the backfill.

3.1 Parametric study

In the present study, the effect of various parameters like horizontal base acceleration, vertical base acceleration,

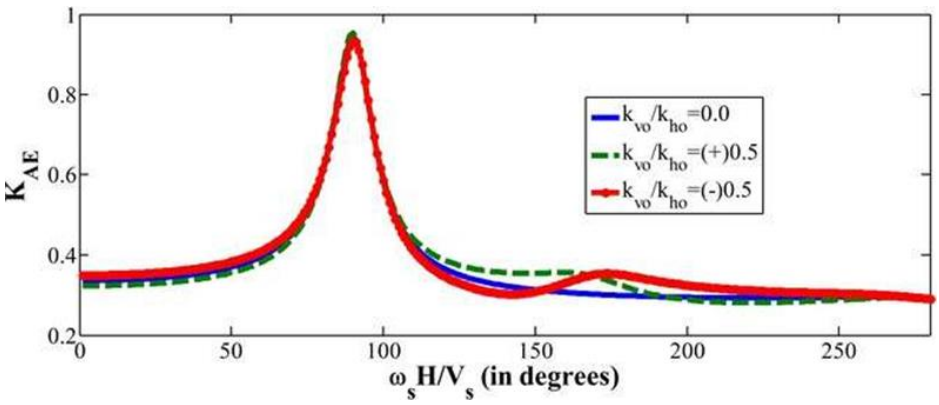

Fig. 9 Effect of primary wave on the formation of peak

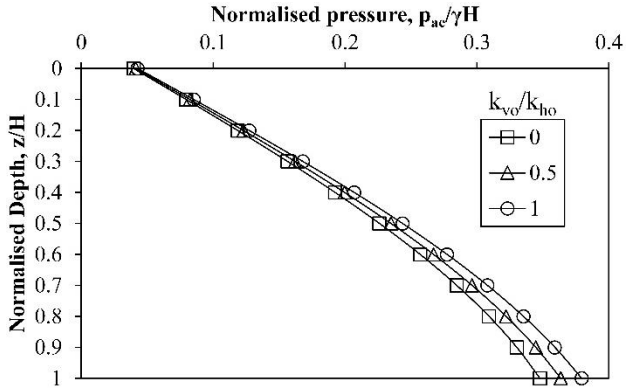

Fig. 10 Seismic active pressure distribution for different vertical base acceleration coefficients

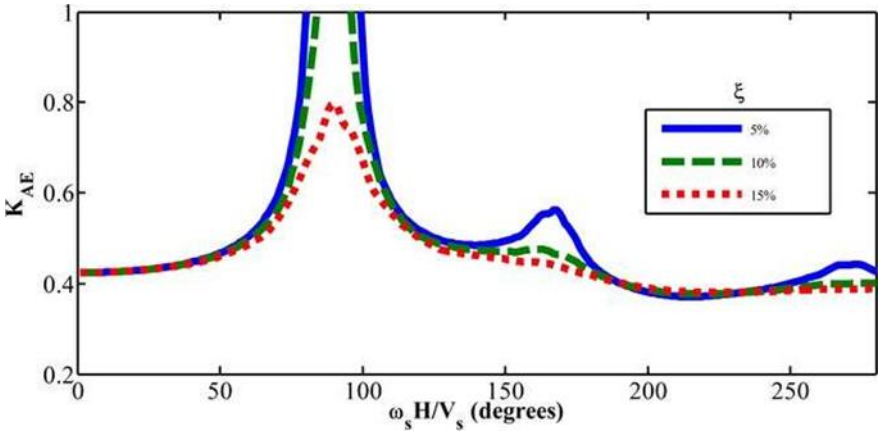

Fig. 11 Effect of Damping ratio on the formation of peak

friction angle, soil-wall friction and wall inclination have been studied as follows.

Influence of horizontal bedrock acceleration

In this section, the effect of k_{ho} on the seismic active thrust is presented in terms of the pressure distribution diagram and the angle made by the failure plane. Fig. 7 shows the influence of the base-acceleration coefficient on lateral earth pressure distribution.

It is observed that as the horizontal base acceleration increases, the non-linearity in the distribution plot increases, including an increase in the magnitude of the pressure. It is observed that the horizontal acceleration coefficient also influences the angle made by the failure plane.

Fig. 8 shows the failure planes generated for different values of the base horizontal acceleration coefficient. The soil mass involved in the failure wedge increases with an increase in k_{ho} as the angle made by the failure plane with vertical increases resulting in an increase in active seismic thrust acting on the wall.

Influence of vertical bedrock acceleration

As the present study considers the propagation of the primary wave, a vertical component of acceleration is assumed at the base, which further amplifies as it reaches the surface of the backfill. Fig. 9 shows the influence of both vertical base acceleration, normalized frequency on the coefficient of seismic earth pressure. In-various other

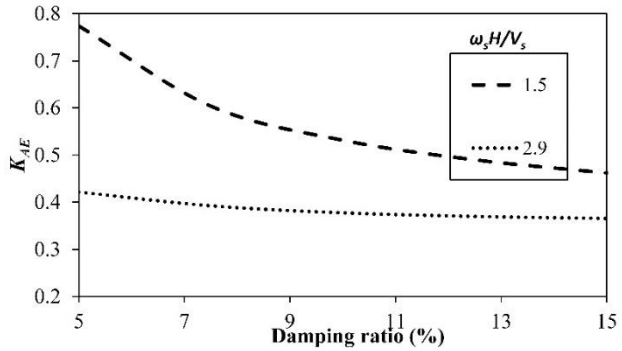

Fig. 12 Effect of Damping ratio on K_{AE} at input frequency ($\omega_s H/V_s$) equal to 1.5 and 2.9

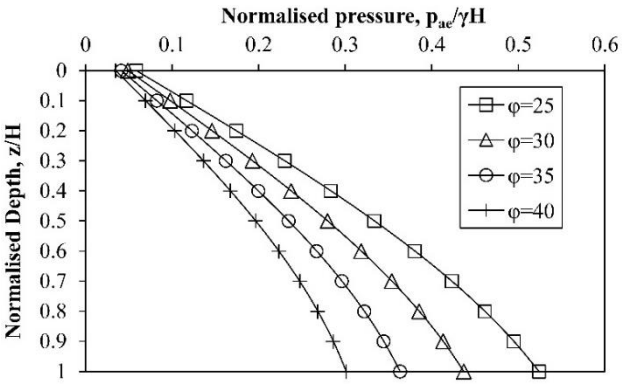

Fig. 13 Seismic earth pressure distribution for different friction angle

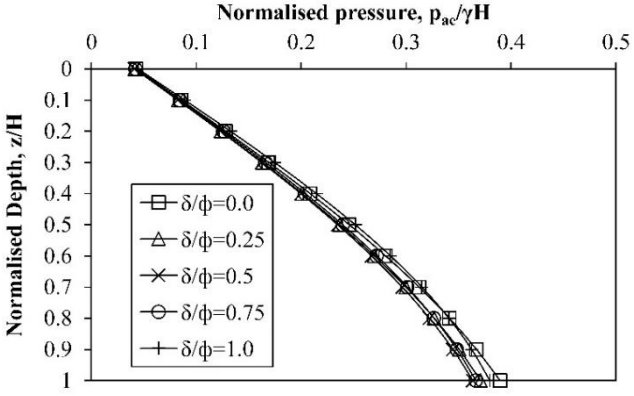

Fig. 14 Seismic earth pressure distribution for different soil-wall friction angles

parameters considered are $\phi = 35^\circ$, $\delta/\phi = 0.5$, $k_{ho} = 0.1$, $n_q = 0.1$, $\xi = 10\%$, $\omega_p = \omega_s$.

The normalized frequency is varied through a range from zero to $3\pi/2$. Similar to Fig. 2, there is a formation of the localized peak in the value of K_{AE} when $\omega_s H/V_s$ is close to $\pi/2$. The formation of the first peak is evident irrespective of the value of the vertical acceleration coefficient. But, there is a formation of the second localized peak that depends on the vertical acceleration coefficient. Second localized peak forms when the $\omega_s H/V_s$ is close to 2.93(167°), i.e., when $\omega_p H/V_p = \pi/2$ which is obtained from the assumptions ($V_p = 1.87V_s$; $\omega_p = \omega_s$). Similar to the first peak, the second peak is also formed as the frequency of the primary wave is close to the fundamental frequency. The magnitude of the second peak is relatively less as it is a known fact that the effect of the shear wave is more compared to that of the primary wave in earth pressure-related problems.

Fig. 10 shows the effect of the vertical base acceleration coefficient on the horizontal earth pressure acting on the height of the retaining wall. The plot considers k_{vo}/k_{ho} values ranging from 0 to 1 with friction angle $\phi = 35^\circ$, soil-wall friction $\delta/\phi = 0.5$, base acceleration coefficient $k_{ho} = 0.1$, normalized frequency of shear wave = 2.0, frequency of primary wave ω_p= frequency of shear wave ω_s and damping resistance of soil $\xi = 10\%$. It is observed that as the ratio k_{vo}/k_{ho} increases, the value of seismic earth pressure also increases. This increase in pressure values is much noticeable at a normalized height (z/H) equal to unity that is at the base of the backfill. At a normalized depth of 1.0, as k_{vo}/k_ho ratio changes from 0.0 to 0.5, seismic earth pressure increases by 4.5% and for k_{vo}/k_{ho} changing from 0.5 to 1.0, the seismic earth pressure increases by 4.3%.

Influence of damping ratio

The major advantage of the present study over existing pseudo-static and pseudo-dynamic methods is the consideration of the damping ratio. Fig. 11 shows the variation of K_{AE} with normalized input frequency for different values of damping ratio. The other parameters considered for the plot are $\phi = 30^\circ$, $\delta/\phi = 0.5$, $k_{ho} = 0.1$, $k_{vo} = 0.5k_{ho}$. It is evident from Fig. 11 that the maximum values of the coefficient are observed when the normalized input frequency of the shear wave is equal to 1.57 and 2.93. For the considered range of input frequency, the damping ratio is effective at these normalized frequencies. Lower the value of the damping ratio, the higher is the peak formed.

Fig. 11 shows the clear formation of peaks at $\omega_s H/V_s = \pi/2(1.5)$ and $\omega_s H/V_s = 2.9$ as explained in previous section. The effect of the damping ratio of backfill to these input frequencies is shown in Fig. 12. It is evident that the damping ratio of backfill soil plays an important role during the formation of the first localized peak compared to that of the second peak as K_{AE} is much sensitive to damping ratio at $\omega_s H/V_s = 1.5$

Influence of internal friction of backfill

Fig. 13 shows the effect of friction angle on seismic earth pressure acting on the wall for the considered values of soil-wall friction $\delta/\phi = 0.5$, base horizontal acceleration coefficient $k_{ho} = 0.1$, base vertical acceleration coefficient $k_{vo} = 0.5k_{ho}$ normalized frequency of shear wave = 2.0, frequency of primary wave ω_p= frequency of shear wave ω_s and damping resistance of soil $\xi = 10\%$. Initially, the lateral pressure at the surface is almost the same for all the considered magnitudes of the friction angle. This initial value mainly depends on the magnitude of the uniform surcharge acting on the surface of the backfill. The value of seismic pressure increases with an increase in the depth of the retaining wall individually for different values of friction angle. As expected, it is evident that as the soil friction angle increases, the seismic pressure decreases. For discussion, as the internal friction angle increases from 25° to 40°, there is a decrease of about 41% in seismic earth pressure at mid-height of the wall and a decrease of about 42.5% at the base of the retaining wall.

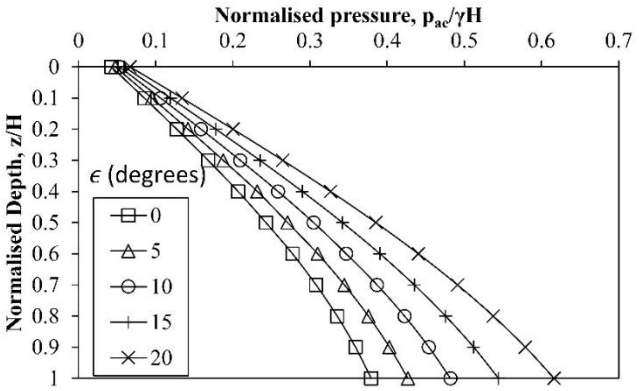

Fig. 15 Seismic earth pressure distribution for different inclinations of the wall back

Table 1 Comparison of seismic earth pressure coefficient with limit equilibrium approach with ξ = 10%, $\omega_s H/V_s$ = 2.356, ω_p/ω_s = 1.0, ϕ = 35°, δ/ϕ = 0.5

kho	Present study	Motta (1994)	Shukla (2013)	Present study	Motta (1994)	Shukla (2013)
		nq=0.0			nq=0.1	
0.0	0.2461	0.2461	0.2461	0.2707	0.2707	0.2707
0.1	0.3237	0.3091	0.2936	0.3598	0.3400	0.3230
0.2	0.4085	0.3987	0.3589	0.4576	0.4385	0.3948
0.3	0.4996	0.5358	0.4554	0.5635	0.5893	0.5009
		n_q = 0.2			n_q = 0.3	
0.0	0.2953	0.2953	0.2953	0.3200	0.3200	0.3200
0.1	0.3958	0.3709	0.3523	0.4319	0.4018	0.3817
0.2	0.5069	0.4785	0.4306	0.5562	0.5184	0.4665
0.3	0.6276	0.6429	0.5465	0.6920	0.6965	0.5920

Table 2 Comparison of seismic earth pressure coefficient with limit analysis with ξ = 10%, $\omega_s H/V_s$ = 2.356, ω_p/ω_s = 1.0, ϕ = 30°, δ/ϕ = 0.5

kho	nq=0.0		nq=0.2		nq=0.3	
	Sahoo and Ganesh (2017)	Present study	Sahoo and Ganesh (2017)	Present study	Sahoo and Ganesh (2017)	Present study
0.1	0.3650	0.3912	0.4375	0.4778	0.5100	0.5644
0.2	0.4535	0.4893	0.5425	0.6062	0.6325	0.7235
0.3	0.5701	0.5952	0.6840	0.7466	0.7950	0.8990

Influence of soil-wall friction

Fig. 14 shows the seismic active pressure distribution on the normalized height of the wall for different values of soil-wall friction angle δ ranging from 0.0 to 1.0 times the friction angle. The other parameters considered are friction angle of soil ϕ = 35°, horizontal base acceleration coefficient k_{ho} = 0.1, vertical base acceleration $k_{vo} = 0.5k_{ho}$, normalized frequency of shear wave $\omega_s H/V_s$ = 2.0, damping ratio ξ = 10%. It is evident that there is a very marginal decrease in the earth-pressure is observed with an increase in soil-wall friction. At the base of the wall (z/H = 1.0), as δ/ϕ changes from 0.0 to 1.0, there is a decrease in earth pressure by 2.5%.

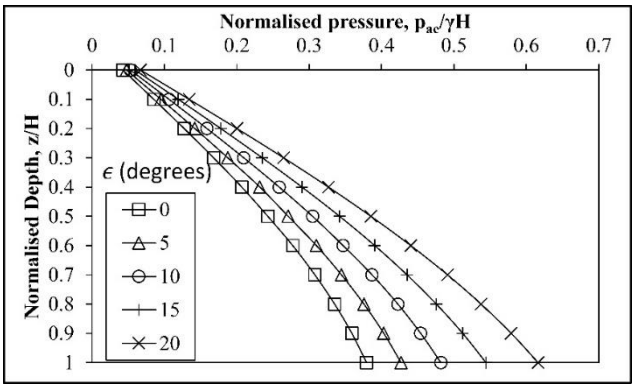

Fig. 15 Seismic earth pressure distribution for different inclinations of the wall back

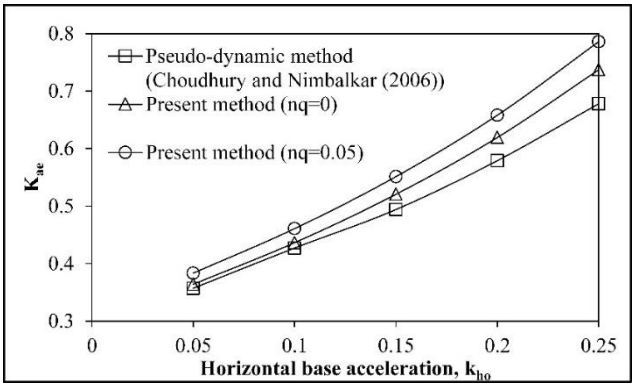

Fig. 16 Comparison of present method with the existing pseudo-dynamic method

Influence of angle made by wall back

The present study includes the effect of non-vertical wall-back on the lateral earth pressure distribution. Fig. 15 shows the pressure distribution on wall varying back-inclination from 0° (vertical) to 20° with vertical. It is observed that as the wall-inclination increases, the magnitude of lateral earth pressure acting on the wall increases. For explanation, when ϵ is varied from 0° to 20°, normalized earth pressure is increased from 0.3795 to 0.6165. This results in an increase of 62.5%. In comparison, this percentage is observed to be 43.4% when the ϵ is varied from 0° to 15°.

3.2 Comparison with existing methods

In this section, the present study is first compared with the existing studies on the pseudo-static method. According to the authors' knowledge, a very limited study was conducted on the effect of surcharge magnitude on the seismic analysis of retaining wall.

The present study is validated using both limit equilibrium analysis and limit analysis. It is found that the proposed study yields an excellent comparison, as shown in Tables (1 and 2). As shown in Table 1, the present study is compared to Motta (1994), Shukla (2013). In comparison, it is observed that at static conditions, the three studies yield the same results. It is observed that though the present study overestimates K_{AE} when compared to Shukla (2013), Sahoo and Ganesh (2017), the values are comparable. Though

there is no specific trend observed when compared to Motta (1994), the obtained values are almost the same. This confirms that the proposed study is valid with its own advantages over existing methods.

An attempt has been made to compare the proposed method with the existing pseudo-dynamic method. Fig. 16 shows a comparison of the coefficient of earth pressure obtained from the existing pseudo-dynamic study and the present study. The set of parameters considered for the comparison are friction angle $\phi = 30^{\circ}$, $\delta/\phi = 0.5$, $\xi = 10\%$, $\omega_s H/V_s = 2.0$, $\omega_p = \omega_s$, $k_{vo} = 0.5k_{ho}$. Due to the lack of pseudo-dynamic studies that dealt with the surcharge on the surface of the backfill, first, it is compared with a no surcharge case ($n_q = 0$), after which a very negligible magnitude of surcharge ($n_q = 0.05$) is considered.

Similar to results obtained from the pseudo-static method, the pseudo-dynamic method also yielded lower values compared to that of the present method for the considered input parameters. The rationale for the higher values of K_{AE} from the present method can be attributed to the non-linear amplification of the acceleration. In the available methods, the amplification is completely neglected (in pseudo-static method) or assumed a linear value (in pseudo-dynamic method). But, in the present methodology, the acceleration amplification is estimated precisely using Eq.(4) and Eq. (6). Apart from the non-linear acceleration profile, another important advantage of the present study is the consideration of damping ratio, which is not considered in pseudo-static and pseudo-dynamic methods. Further, with a small increase in surcharge coefficient, a small increase in K_{AE} is observed, as shown in Fig. 16.

The present study advances the concept of seismic analysis of rigid retaining walls by considering the time dependency, amplification of acceleration in the backfill considering dynamic properties of soil, input frequency of the shear wave, primary wave, and uniform surcharge over the surface of the backfill. This methodology can also be extended to other types of retaining walls like cantilever retaining walls where the corresponding failure mechanism (Kamiloğlu and Şadoğlu (2017), Alper Kamiloğlu and Sadoğlu (2019), Greco (2001)) is assumed with proposed acceleration profiles to estimate inertial forces. The present study also has some limitations for the application. The proposed study considers linear values of damping ratio and shear modulus, whereas, in reality, the damping ratio increases and shear modulus decreases with increasing shear strain during dynamic action (Seed and Idriss (1970)). Therefore the present study is applicable for low to medium seismic acceleration coefficients (k_{ho} and k_{vo}). For higher seismic coefficients, the non-linearity plays a crucial role and present values may not be suitable. The present study is applicable for a uniform surcharge on the horizontal backfill surface. The boundary constraints have to be changed accordingly for the inclined surcharge case. The proposed study is applicable when the soil-wall system is resting on a rigid base. In some cases, the soil-wall system rests on a foundation soil, where the amplification of acceleration should also be considered. The basic soil properties like friction angle.

4. Conclusions

The present study proposes a more generalized modified pseudo-dynamic method to estimate active seismic pressure acting on the retaining wall with surcharged backfill. The amplification of shear wave, primary wave are considered in estimating the inertial force due to potential soil wedge and surcharge. The boundary constraints due to uniform surcharge at the surface of the backfill are satisfied. In addition, the proposed method is found to be in good agreement with the existing pseudo-static and pseudo-dynamic methods. Apart from the mentioned advantages, the study yields the following conclusions:

1. The deduced acceleration equations show that the amplification of the upward propagating shear wave and primary wave depends on the dynamic properties of the backfill soil and is not affected by the magnitude of the uniform surcharge.

2. It is observed that the maximum value of the seismic active pressure coefficient is obtained when normalized input frequency $\omega_s H/V_s$ is equal to $\pi/2$. For the assumed velocity and frequency of the primary wave, the second and relatively smaller peak is formed when $\omega_p H/V_p$ is equal to $\pi/2$.

3. The maximum horizontal inertial force and vertical inertial forces acting on the potential failure wedge and uniform surcharge occur at different times of the seismic event.

4. For the considered input frequency, the present method yields a higher coefficient of seismic earth pressure compared to that of the pseudo-static and pseudo-dynamic methods. This can be attributed to a non-linear amplification of acceleration considered in the present study. In pseudo-static methods, the amplification is totally neglected, whereas a linear acceleration is considered in pseudo-dynamic methods.

The proposed methods can definitely answer the question related to seismic earth pressure with sur- charged backfill and yield a reliable value of K_{AE} for a safe design of retaining wall against destructive earthquakes.

References

Alper Kamiloğlu, H., and Sadoğlu, E. (2019), "Experimental and theoretical investigation of short-and long-heel cases of cantilever retaining walls in active state", *Int. J. Geomech*., **19**(5), 04019023. https://doi.org/10.1061/(ASCE)GM.1943-5622.0001389

Aminpour, M.M., Maleki, M., and Ghanbari, A. (2017), "Investigation of the effect of surcharge on behavior of soil slopes", *Geomech. Eng*., **13**(4), 653-669. https://doi.org/10.12989/gae.2017.13.4.653

Annapareddy, V.R. and Pain, A. (2019), "Effect of strain-dependent dynamic properties of backfill and foundation soil on the external stability of geosynthetic reinforced waterfront retaining structure subjected to harmonic motion", *Appl. Ocean Res*., **91**, 101899, https://doi.org/10.1016/j.apor.2019.101899.

Baziar, M. H., Shahnazari, H. and Rabeti Moghadam, M. (2013), "Sliding stability analysis of gravity retaining walls using the pseudo-dynamic method", *Proc. Inst. Civ. Eng. Geotech. Eng*., **166**(4), 389-398, https://doi.org/10.1680/geng.10.00036.

Bellezza, I. (2014), "A new pseudo-dynamic approach for seismic active soil thrust", *Geotech. Geol. Eng.*, **32**(2), 561-576. https://doi.org/10.1007/s10706-014-9734-y.

Cakir, T. (2013), "Evaluation of the effect of earthquake frequency content on seismic behavior of cantilever retaining wall including soil–structure interaction", *Soil Dyn. Earthq. Eng.*, **45**, 96-111. https://doi.org/10.1016/j.soildyn.2012.11.008.

Cakir, T. (2014a), "Backfill and subsoil interaction effects on seismic behavior of a cantilever wall", *Geomech. Eng.*, **6**(2), 117-138. http://doi.org/10.12989/gae.2014.6.2.117.

Cakir, T. (2014b), "Influence of wall flexibility on dynamic response of cantilever retaining walls", *Struct. Eng. Mech.*, **49**(1), 1-22, http://doi.org/10.12989/sem.2014.49.1.001.

Cakir, T. (2017), "Assessment of effect of material properties on seismic response of a cantilever wall", *Geomech. Eng.*, **13**(4), 601-619, https://doi.org/10.12989/gae.2017.13.4.601.

Cakir, T. and Livaoglu, R. (2013), "Experimental analysis on FEM definition of backfill-rectangular tank-fluid system", *Geomech. Eng.*, **5**(2), 165-185, https://doi.org/10.12989/gae.2013.5.2.165.

altabiano, S., Cascone, E. and Maugeri, M. (2000), "Seismic stability of retaining walls with sur- charge", *Soil Dyn. Earthq. Eng.*, **20**(5-8), 469-476. https://doi.org/10.1016/S0267- 7261(00)00093-2.

Choudhury, D. and Nimbalkar, S.S. (2006), "Pseudo-dynamic approach of seismic active earth pressure behind retaining wall", *Geotech. Geol. Eng.*, **24**(5), 1103. https://doi.org/10.1007/s10706- 005-1134-x

Choudhury, D. and Rao, K.S.S (2002), "Seismic passive resistance in soils for negative wall friction", *Can. Geotech. J.*, **39**(4), 971-981, https://doi.org/10.1139/t02-023.

Choudhury, D., and Nimbalkar, S. (2007), "Seismic rotational displacement of gravity walls by pseudo- dynamic method: Passive case", *Soil Dyn. Earthq. Eng.*, **27**(3), 242-249. https://doi.org/10.1016/j.soildyn.2006.06.009.

di Santolo, A.S. and Evangelista, A. (2011), "Dynamic active earth pressure on cantilever retaining walls", *Comput. Geotech.*, **38**(8), 1041-1051, https://doi.org/10.1016/j.compgeo.2011.07.015.

Das, B.M. (1993), *Principles of Soil Dynamics*, Kent Publishing Company, Boston, Massachusetts, U.S.A.

Evangelista, A., di Santolo, A.S. and Simonelli (2010), "Evaluation of pseudostatic active earth pressure coefficient of cantilever retaining walls", *Soil Dyn. Earthq. Eng.*, **30**(11), 1119- 1128. https://doi.org/10.1016/j.soildyn.2010.06.018.

Gazetas, G., Psarropoulos, P. N., Anastasopoulos, I. and Gerolymos, N. (2004), "Seismic behaviour of flexible retaining systems subjected to short-duration moderately strong excitation", *Soil Dyn. Earthq. Eng.*, **24**(7), 537-550. https://doi.org/10.1016/j.soildyn.2004.02.005.

Ghanbari, A., and Ahmadabadi, M. (2010), "Pseudo-dynamic active earth pressure analysis of inclined retain- ing walls using horizontal slices method", *Scientia Iranica Trans. A Civ. Eng.*, **17**(2), 118-130.

Ghosh, P. (2008), "Seismic active earth pressure behind a nonvertical retaining wall using pseudo-dynamic analysis", *Can. Geotech. J.*, **45**(1), 117-123. https://doi.org/10.1139/T07-071

Ghosh, S. (2010), "Pseudo-dynamic active force and pressure behind battered retaining wall sup- porting inclined backfill", *Soil Dyn. Earthq. Eng.*, **30**(11), 1226-1232. https://doi.org/10.1016/j.soildyn.2010.05.003.

Giarlelis, C. and Mylonakis, G. (2011), "Interpretation of dynamic retaining wall model tests in light of elastic and plastic solutions", *Soil Dyn. Earthq. Eng.*, **31**(1), 16-24. https://doi.org/10.1016/j.soildyn.2010.07.002.

Greco, V. (2001), "Active earth thrust on cantilever walls with short heel", *Can. Geotech. J.*, **38**(2), 401-409. https://doi.org/10.1139/t00-094.

Greco, V. (2006), "Active thrust due to backfill subject to lines of surcharge", *J. Geotech. Geoenviron. Eng.*, **132**(2), 269-271. https://doi.org/10.1061/(ASCE)1090- 0241(2006)132:2(269).

Hu, H. and Huang, Y. (2019), "A dynamic reliability approach to seismic vulnerability analysis of earth dams", *Geomech. Eng.*, **18**(6), 661-668, https://doi.org/10.12989/gae.2019.18.6.661.

Huang, D. and Liu, J. (2016), "Upper-bound limit analysis on seismic rotational stability of retaining wall", *KSCE J. Civ. Eng.*, **20**(7), 2664-2669. https://doi.org/10.1007/s12205-016-0471-z.

Kamiloğlu, H.A. and Şadoğlu, E. (2017), "Active earth thrust theory for horizontal granular backfill on a cantilever wall with a short heel", *Int. J. Geomech.*, **17**(8), 04017018. https://doi.org/10.1061/(ASCE)GM.1943-5622.0000886

Kloukinas, P., di Santolo, A.S., Penna, A., Dietz, M., Evangelista, A., Simonelli, A.L., Taylor, C. and Mylonakis, G. (2015), "Investigation of seismic response of cantilever retaining walls: Limit analysis vs shaking table testing", *Soil Dyn. Earthq. Eng.*, **77**, 432-445. https://doi.org/10.1016/j.soildyn.2015.05.018

Kolathayar, S and Ghosh, P. (2009), "Seismic active earth pressure on walls with bilinear backface using pseudo-dynamic approach", *Comput. Geotech.*, **36**(7), 1229-1236. https://doi.org/10.1016/j.compgeo.2009.05.015.

Kramer, S.L. (1996), *Geotechnical Earthquake Engineering*, Pearson Education India.

Kumar, J. and Chitikela, S (2002), "Seismic passive earth pressure coefficients using the method of characteristics", *Can. Geotech. J.*, **39**(2), pp. 463-471, https://doi.org/10.1139/t01-103.

Madabhushi, S.P.G. and Zeng, X. (2007), "Simulating seismic response of cantilever retaining walls", *J. Geotech. Geoenviron. Eng.*, **133**(5), 539-549. https://doi.org/10.1061/(ASCE)1090-0241(2007)133:5(539).

Mononobe, N. and Matsuo, H. (1929), "On the determination of earth pressures during earthquakes", *Proceedings of the World Engineering Congress*, Tokyo, Japan.

Motta, E. (1994), "Generalized Coulomb active-earth pressure for distanced surcharge", *J. Geotech. Eng.*, **120**(6), 1072-1079. https://doi.org/10.1061/(ASCE)0733-9410(1994)120:6(1072).

Motlagh, A.T., Ghanbari, A., Maedeh, P.A. and Wu, W. (2018), "A new analytical approach to estimate the seismic tensile force of geosynthetic reinforcement respect to the uniform surcharge of slopes", *Earthq. Struct.*, **15**(6), 687-699. https://doi.org/10.12989/eas.2018.15.6.687.

Mylonakis, G., Kloukinas, P. and Papantonopoulos, C. (2007), "An alternative to the Mononobe–Okabe equations for seismic earth pressures", *Soil Dyn. Earthq. Eng.*, **22**(10), 947-969. https://doi.org/10.1016/j.soildyn.2007.01.004.

Nimbalkar, S., and Choudhury, D. (2007), "Sliding stability and seismic design of retaining wall by pseudo- dynamic method for passive case", *Soil Dyn. Earthq. Eng.*, **27**(6), 497-505. https://doi.org/10.1016/j.soildyn.2006.11.006.

Okabe, S. (1924), "General theory on earth pressure and seismic stability of retaining wall and dam", *Proc. Civ. Eng. Soc.*, **10**(6), 1277-1323.

Pain, A., Annapareddy, V.S. and Nimbalkar, S. (2018), "Seismic active thrust on rigid retaining wall using strain dependent dynamic properties", *Int. J. Geomech.*, **18**(12), 06018034. https://doi.org/10.1061/(ASCE)GM.1943-5622.0001331.

Pain, A., Choudhury, D. and Bhattacharyya, S.K. (2017), "Seismic rotational stability of gravity retaining walls by modified pseudo-dynamic method", *Soil Dyn. Earthq. Eng.*, **94**, 244-253. https://doi.org/10.1016/j.soildyn.2017.01.016.

Psarropoulos, P.N., Klonaris, G. and Gazetas, G. (2005), "Seismic earth pressures on rigid and flexible retaining walls", *Soil Dyn. Earthq. Eng.*, **25**(7-10), 795-809.

https://doi.org/10.1016/j.soildyn.2004.11.020.
Qin, C. and Chian, S.C. (2018), "External stability of reinforced soil walls under seismic conditions", *Comput. Geotech.*, **102**, 196-205. https://doi.org/10.1680/gein.2007.14.4.211.
Richards Jr, R. and Elms, D.G., (1979), "Seismic behavior of gravity retaining walls", *J. Geotech. Geoenviron. Eng.*, **105**(4), 449-464. https://doi.org/10.1061/AJGEB6.0000783.
Santhoshkumar, G. and Ghosh, P. (2018), "Seismic passive earth pressure on an inclined cantilever retaining wall using method of stress characteristics–A new approach", *Soil Dyn. Earthq. Eng.*, **107**, 77-82. https://doi.org/10.1016/j.soildyn.2018.01.021.
Santhoshkumar, G and Ghosh, P. (2020), "Seismic stability of a broken-back retaining wall using adaptive collapse mechanism", *Int. J. Geomech.*, **20**(9), 04020154. https://doi.org/10.1061/(ASCE)GM.1943-5622.0001786
Sahoo, J.P. and Ganesh, R. (2017), "Kinematic limit analysis approach for seismic active earth thrust co-efficients of cohesive-frictional backfill", *Int. J. Geomech.*, **18**(1), 04017123. https://doi.org/10.1061/(ASCE)GM.1943-5622.0001030.
Seed, H and Idriss, I.M. (1970), "Soil moduli and damping factors for dynamic response analyses", Report No. Centre report UCB/EERC-70/10, Earthquake Engineering Research Center, University of California, Berkeley, California, U.S.A.
Shukla, S.K. (2013), "Seismic active earth pressure from the sloping c-ϕ soil backfills", *Indian Geotech. J.*, **43**(3), 274-279. https://doi.org/10.1007/s40098-013-0044-8.
Srikar, G. and Mittal, S. (2020), "Seismic analysis of retaining wall subjected to surcharge: A modified pseudodynamic approach", *Int. J. Geomech.*, **20**(9), 06020022. https://doi.org/10.1061/(ASCE)GM.1943-5622.0001780.
Steedman, R.S. and Zeng, X. (1990), "The influence of phase on the calculation of pseudo-static earth pressure on a retaining wall", *Geotechnique*, **40**(1), 103-112. https://doi.org/10.1680/geot.1990.40.1.103.
Taravati, H. and Ardakani, A. (2018), "The numerical study of seismic behavior of gravity retaining wall built near rock face", *Earthq. Struct.*, **14**(2), 179-186. https://doi.org/10.12989/eas.2018.14.2.179.
Veletsos, A. and Younan, A.H. (1994a), "Dynamic modeling and response of soil-wall systems", *J. Geotech. Eng.*, **120**(12), 2155-2179. https://doi.org/10.1061/(ASCE)0733- 9410(1994)120:12(2155).
Veletsos, A. and Younan, A.H. (1994b), "Dynamic soil pressures on rigid vertical walls", *Earthq. Eng. Struct. Dyn.*, **23**(3), 275-301. https://doi.org/10.1002/eqe.4290230305.
Veletsos, A. and Younan, A.H. (1997), "Dynamic response of cantilever retaining walls", *J. Geotech. Geoenviron. Eng.*, **123**(2), 161-172. https://doi.org/10.1061/(ASCE)1090- 0241(1997)123:2(161).
Wang, J.J., Zhang, H.P., Chai, H.J. and and Zhu, J.G. (2008), "Seismic passive resistance with vertical seepage and surcharge", *Soil Dyn. Earthq. Eng.*, **28**(9), 728-737. https://doi.org/10.1016/j.soildyn.2007.10.004.
Zhang, D.B., Jiang, Y. and Yang, X.L. (2019), "Estimation of 3D active earth pressure un- der nonlinear strength condition", *Geomech. Eng.*, **17**(6), 515-525. https://doi.org/10.12989/gae.2019.17.6.515

Appendix

A.1 Terms used in horizontal acceleration and horizontal displacement

$$X=\frac{Hq\tan\phi}{G\left(y_{s1}^2+y_{s2}^2\right)\left(U_s^{\,2}+V_s^{\,2}\right)}\begin{bmatrix} y_{s1}\begin{pmatrix}\left\{U_{sz}V_s-V_{sz}U_s\right\}N_s-\left\{U_{sz}U_s+V_{sz}V_s\right\}M_s\\ +\left\{U_s^{\,2}+V_s^{\,2}\right\}M_{sz}\end{pmatrix}\\ +y_{s2}\begin{pmatrix}\left\{V_{sz}U_s-U_{sz}V_s\right\}M_s-\left\{U_{sz}U_s+V_{sz}V_s\right\}N_s\\ +\left\{U_s^{\,2}+V_s^{\,2}\right\}N_{sz}\end{pmatrix}\end{bmatrix} \quad (14)$$

$$N_s=\cos\left(y_{s1}\right)\sinh\left(y_{s2}\right) \quad (15)$$

$$M_s=-\sin\left(y_{s1}\right)\cosh\left(y_{s2}\right) \quad (16)$$

$$N_{sz}=\cos\left(y_{s1}z/H\right)\sinh\left(y_{s2}z/H\right) \quad (17)$$

$$M_{sz}=-\sin\left(y_{s1}z/H\right)\cosh\left(y_{s2}z/H\right) \quad (18)$$

$$U_{sz}=\cos\left(y_{s1}z/H\right)\cosh\left(y_{s2}z/H\right) \quad (19)$$

$$V_{sz}=-\sin\left(y_{s1}z/H\right)\sinh\left(y_{s2}z/H\right) \quad (20)$$

$$U_s=\cos\left(y_{s1}\right)\cosh\left(y_{s2}\right) \quad (21)$$

$$V_s=-\sin\left(y_{s1}\right)\sinh\left(y_{s2}\right) \quad (22)$$

$$y_{s1}=\frac{\omega_s H}{V_s}\sqrt{\frac{\sqrt{1+4\xi_s^{\,2}}+1}{2\left(1+4\xi_s^{\,2}\right)}} \quad (23)$$

$$y_{s2}=\frac{\omega_s H}{V_s}\sqrt{\frac{\sqrt{1+4\xi_s^{\,2}}-1}{2\left(1+4\xi_s^{\,2}\right)}} \quad (24)$$

A.2 Terms used in vertical acceleration and vertical displacement

$$Y=\frac{Hq}{M\left(y_{p1}^2+y_{p2}^2\right)\left(U_p^{\,2}+V_p^{\,2}\right)}\begin{bmatrix} y_{p1}\begin{pmatrix}\left\{U_{pz}V_p-V_{pz}U_p\right\}N_p-\left\{U_{pz}U_p+V_{pz}V_p\right\}M_p\\ +\left\{U_p^{\,2}+V_p^{\,2}\right\}M_{pz}\end{pmatrix}\\ +y_{p2}\begin{pmatrix}\left\{V_{pz}U_p-U_{pz}V_p\right\}M_p-\left\{U_{pz}U_p+V_{pz}V_p\right\}N_p\\ +\left\{U_p^{\,2}+V_p^{\,2}\right\}N_{pz}\end{pmatrix}\end{bmatrix} \quad (25)$$

$$N_p=\cos\left(y_{p1}\right)\sinh\left(y_{p2}\right) \quad (26)$$

$$M_p=-\sin\left(y_{p1}\right)\cosh\left(y_{p2}\right) \quad (27)$$

$$N_{pz}=\cos\left(y_{p1}z/H\right)\sinh\left(y_{p2}z/H\right) \quad (28)$$

$$M_{pz}=-\sin\left(y_{p1}z/H\right)\cosh\left(y_{p2}z/H\right) \quad (29)$$

$$U_{pz}=\cos\left(y_{p1}z/H\right)\cosh\left(y_{p2}z/H\right) \quad (30)$$

$$V_{pz}=-\sin\left(y_{p1}z/H\right)\sinh\left(y_{p2}z/H\right) \quad (31)$$

$$U_p=\cos\left(y_{p1}\right)\cosh\left(y_{p2}\right) \quad (32)$$

$$V_p=-\sin\left(y_{p1}\right)\sinh\left(y_{p2}\right) \quad (33)$$

$$y_{p1}=\frac{\omega_p H}{V_p}\sqrt{\frac{\sqrt{1+4\xi_p^{\,2}}+1}{2\left(1+4\xi_p^{\,2}\right)}} \quad (34)$$

$$y_{p2}=\frac{\omega_p H}{V_p}\sqrt{\frac{\sqrt{1+4\xi_p^{\,2}}-1}{2\left(1+4\xi_p^{\,2}\right)}} \quad (35)$$